RSC Advances

PAPER

View Article Online
View Journal | View Issue

Cite this: *RSC Adv.*, 2025, **15**, 29176

Efficient and selective leaching of nickel and cobalt from nickel laterite ore by a combined atmospheric acid leaching-ferric chloride solution leaching process: optimization and mechanism

Jingbei Li,[a] Tong Yu,[a] Chenyang Li,[a] Xiao Han[a] and Jianming Gao *[ab]

Low-selectivity leaching of nickel and/or cobalt is a major problem for atmospheric acid leaching processes, while harsh leaching conditions make the pressurised acid leaching process costly. Thus, the development of an efficient and selective leaching process of cobalt and nickel under mild conditions is required. Here, a combined atmospheric acid leaching-ferric chloride solution leaching process was developed to leach cobalt and nickel selectively and efficiently over iron from nickeliferous laterite ores. The influences of leaching parameters on the leaching efficiency of valuable metals during the atmospheric acid and ferric chloride solution leaching processes were investigated, and the overall recovery was also calculated and analyzed. Under the optimized leaching conditions, the leaching efficiencies of Ni, Co and Mn besides Fe could reach more than 95.0% after the atmospheric acid leaching process, with the Fe^{3+} concentration varying from 62.0 g L^{-1} to 157 g L^{-1} in the leach liquors. After the ferric chloride solution leaching process at 180 °C for 120 min using the initial leach liquors with iron concentrations of 160 and 100 g L^{-1}, the leaching efficiencies of Ni, Mn, Co, and Mg were around 90.0%, while the precipitation efficiencies of iron were 89.0% and 90.5% for saprolite and limonite laterite ore, respectively. Efficient and selective leaching of valuable metals from limonite and saprolite laterite ore under mild conditions was thus realized using the proposed process.

Received 23rd June 2025
Accepted 4th August 2025

DOI: 10.1039/d5ra04469c

rsc.li/rsc-advances

1. Introduction

Nickel (Ni) is widely used in fields such as stainless steel,[1] catalysis,[2] magnetic materials,[3] and lithium-ion batteries,[4] and it is found predominantly in the nickeliferous sulfide ore (30%) and nickeliferous laterite ore (70%). Over the past few decades, nickel sulfide ore has been enriched at low cost, and high-grade sulfide ore became the main source of nickel in the world. However, with the decrease in the available nickel sulfide ore resources and the increasing demand for nickel metal, the nickeliferous laterite ore has become the primary nickel resource. Nickel laterite ore is an associated resource containing nickel, cobalt, manganese, magnesium, and iron, and it can be classified into limonite, transition, and saprolite laterite ores, according to the characteristics of the mineral phase and the chemical composition.[5] It is worth noting that cobalt (Co), as one of the most important strategic metals, is widely used in batteries,[6] catalysis,[7] pigments,[8] and alloys.[9] Generally, limonite laterite is relatively rich in cobalt, while saprolite laterite ore is relatively rich in nickel. As a result, it is important and meaningful to selectively extract Ni and Co from both saprolite and limonite laterite ore for the sustainable supply of strategic metals and efficient utilization of these mineral resources.

Among the metallurgical processes for nickeliferous laterite ore, acid leaching, including pressure acid leaching[10] and atmospheric acid leaching processes,[11] is an effective method that has attracted considerable interest in recent years. Generally, high leaching efficiencies of Ni and Co (above 90%) with high selectivity for Ni and Co over Fe can be realized using the pressure acid leaching process. However, the harsh leaching conditions (250–270 °C and 4–5 MPa) required for the pressure acid leaching process[12] require specialized material reactors with high corrosion resistance, such as titanium-lined autoclaves, which makes the process costly. In contrast, the atmospheric acid leaching process can leach valuable metals from nickeliferous laterite ore under mild conditions, with lower energy consumption and simpler operation.[13,14] However, it is worth noting that a large amount of impurity metal ions, especially Fe^{3+} ions, coexist in the leach liquor, resulting in a complex purification–separation processes and associated nickel/cobalt losses.[15–17] Although these leaching processes have been applied in industry, their shortcomings and problems limit further development of the processes or increase the cost

[a]*Institute of Resources and Environment Engineering, Shanxi University, Taiyuan 030006, P. R. China. E-mail: gaojianming@sxu.edu.cn*

[b]*Shanxi Key Laboratory of High Value Recycling of Coal Based Solid Waste, Shanxi Laboratory for Yellow River, Shanxi University, Taiyuan, 030006, China*

of production. Consequently, it is desirable to develop a highly efficient and selective leaching technology for nickel extraction from nickeliferous laterite ore under mild leaching conditions.

To solve the problems outlined above, several studies have been conducted to enhance the leaching process or improve the leaching selectivity for Ni and Co extraction from nickeliferous laterite ore. Various approaches, including pretreatment or activation of raw laterite ore,[18,19] intensified heating methods,[20] and the addition of reducing[21] or surface-active agents,[22] have been reported to enhance the atmospheric acid leaching process. For laterite ores, most of the nickel is isomorphically substituted into serpentine ($Mg_3Si_2O_5(OH)_4$) or goethite (FeOOH). To expose nickel from the stable crystal structures, activation pretreatment of the laterite ore, such as through thermal, mechanical or chemical activation, has been used, and the metal leaching efficiency has either been improved or the leaching time has been decreased. Compared to conventional heating methods, microwave heating is more effective, uniform and faster, leading to enhanced leaching efficiency of valuable metals and shortening the leaching time. In addition, adding SO_2 and Cu ions as reducing agents or stearyl trimethyl ammonium chloride (STAC) as a surface-active agent to the leaching solution can improve the leaching rate and decrease the leaching time. Generally, the leaching efficiency can be improved and the leaching time can be reduced using the above methods. However, it should be noted that the leaching efficiency for all the metals, including iron and magnesium, can be enhanced, resulting in poor leaching selectivity for nickel and cobalt extraction. For example, it has been reported that although only approximately 20% of the iron could be leached into the liquor when ammonia chloride was added to the hydrochloric acid leaching solution,[23] it is difficult to further decrease the iron leaching efficiency using this method. Therefore, selective leaching and high-efficiency extraction of Ni and Co from laterite ore in a cost-effective way have become key issues and pose a challenge that needs to be addressed.

Considering the advantages of both atmospheric and pressure acid leaching processes, a new combined atmospheric acid leaching-ferric chloride leaching process to leach Ni and Co selectively and efficiently from nickeliferous laterite ore is developed in this study. First, valuable metals, including Ni, Mn, Co, and Mg, in addition to Fe, are leached from limonite laterite ore through the atmospheric acid leaching process. The leach liquors with high concentrations of Fe^{3+} ions are then used as the leaching agent for saprolite or limonite laterite ore. Thus, nickel and cobalt are leached from saprolite or limonite laterite ore by hydrogen ions, which are generated from the hydrolysis of Fe^{3+} ions in the leach liquor. In this way, high-efficiency leaching of Ni and Co from both limonite and saprolite laterite ores with high selectively over Fe was obtained; at the same time, the residual acid was effectively utilized and acid consumption was greatly reduced. In this study, the metal leaching behavior from limonite laterite ore during the atmospheric acid leaching process and from saprolite or limonite laterite ores during the ferric chloride solution leaching process, were systematically investigated. Leaching mechanisms for the combined process are proposed. Moreover, the migration and transformation behavior for each metal is summarized, and the overall recoveries are reported. This paper thus describes a mild and efficient leaching technology for metal recovery from nickeliferous laterite ore of various types.

2. Experimental

2.1 Materials and reagents

The nickeliferous laterite ores of limonite and saprolite type used in the present paper were obtained from China ENFI Engineering Technology Co., Ltd. The laterite ores were dried at 110 °C for 24 h, and then ground into uniform powders (150 mesh). Analytically pure concentrated hydrochloric acid solution and $FeCl_3 \cdot 6H_2O$ were purchased from Sinopharm Chemical Reagent Co., Ltd and used without pretreatment.

2.2 Experimental procedure

Fig. 1 presents a flowchart for the ambient-pressure acid leaching-ferric chloride solution extraction of nickel and cobalt from limonitic bauxite and lateritic ore. The process consists of two stages: (1) ambient-pressure acid leaching of limonitic bauxite; and (2) ferric chloride solution leaching of saprolitic or limonitic ore. To establish a closed-loop $FeCl_3$–HCl system, the Fe^{3+} and HCl concentrations in the leaching liquors can be restored to the initial concentrations by replenishing $FeCl_3$ and hydrochloric acid, enabling reuse cycles with minimal loss in Ni and Co recovery efficiencies. Finally, the spent leachate is treated to remove residual Fe^{3+}, Cl^-, and trace Ni^{2+}/Co^{2+}, ensuring that effluent quality meets Integrated Wastewater Discharge Standard (GB 8978-1996) and related environmental regulations. This significantly reduces the consumption of raw

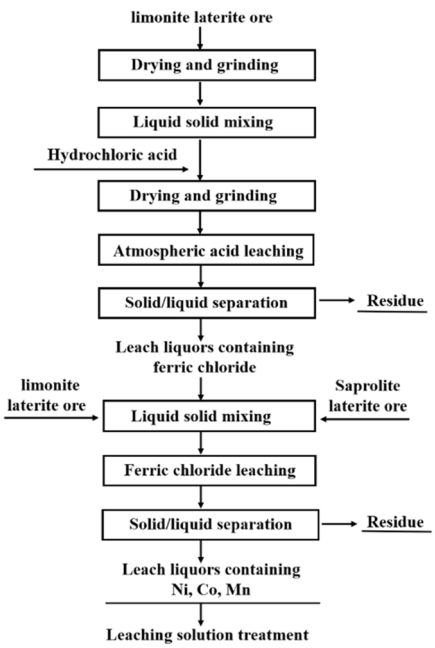

Fig. 1 Flow sheet for efficient and selective leaching of Ni and Co from limonite and saprolite laterite ore by the atmospheric acid leaching-ferric chloride leaching combined process.

materials and improves the economic viability and environmental friendliness of the process.

2.2.1 Atmospheric acid leaching process. The limonite laterite ore was mixed with defined concentrations of HCl solution (3, 4, 4.8, 6 and 8 mol L^{-1}) in a 500 mL glass reactor at a given solid–liquid ratio (1 : 8, 1 : 6, 1 : 5, 1 : 4 and 1 : 3 g mL^{-1}), and then the mixture was heated to reflux and reacted at the designated temperature (increasing from 30–100 °C) for a given time (varying from 20–90 min) with magnetic stirring. Upon completion of leaching, liquid–solid separation was conducted using a high-speed centrifuge at 4500 rpm. The leach residue was washed three times with deionized water, and then dried at 105 °C for analysis of the chemical and phase compositions. In addition, samples of leach liquor were collected to analyze the concentration of valuable metals using an inductively coupled plasma atomic emission spectrometer (ICP-AES, Varian, America) and determine the leaching efficiency for each metal.

2.2.2 Ferric chloride solution leaching process. The saprolite or limonite laterite ore was mixed in a 100 mL Teflon tank with a defined concentration of $FeCl_3$ solution (varying from 60 to 160 g L^{-1}) or acid leach liquors produced from the atmospheric acid leaching of limonite laterite ore at the given liquid–solid ratio (increasing from 0.8 to 1.2 mL g^{-1}). The Teflon-lined tank was then sealed inside a stainless autoclave and fixed in a homogeneous reactor with precise temperature control. The mixture was reacted for 180 min at the designed leaching temperature (increasing from 120 °C to 200 °C) with uniform rotation. When the leaching process was complete, the obtained leach slurry was cooled to room temperature in the reactor and then separated by suction filtration. The leach residue was washed three times with deionized water and dried at 105 °C for analysis of the chemical and phase compositions. The leach liquor was collected to analyze the concentration of metal ions by ICP-AES. Significantly, this series of experiments initially used synthetic liquors to study the change of leaching efficiency and precipitation efficiency of Fe^{3+} with leaching conditions; subsequent studies focused on the use of real leach liquors selected from the atmospheric acid leaching process for verification.

2.3 Characterization and analysis

The chemical compositions of two kinds of nickeliferous laterite ores and leach residues were measured using X-ray fluorescence (XRF-S8 TIGER, Bruker, Germany). Their mineral phase compositions were recorded using an X-ray diffractometer (XRD-Rigaku, Japan) with Cu Kα radiation ($\lambda = 0.15406$ nm) at a scanning rate of 0.02° s^{-1} in the diffraction angle (2θ) of 10° to 90°. The concentrations of metal ions in the leach liquors were determined with an inductively coupled plasma atomic emission spectrometer (ICP-AES, Varian, America). The residual acid concentrations in the leaching liquors were measured with a pH meter (PHS-3C, China).

2.4 Calculation of metal extraction

The leaching efficiency η_1 of each valuable metal, apart from Fe^{3+} ions, during the atmospheric acid leaching process of limonite laterite ore and the leaching efficiency η_2 of each metal except Fe^{3+} ions using $FeCl_3 \cdot 6H_2O$ solution as lixiviant during the ferric chloride solution leaching process of saprolite or limonite laterite ore were calculated according to eqn (1).

$$\eta_1 = \eta_2 = \frac{C_x V_c}{M W_X} \times 100\% \quad (1)$$

where C_X represents the concentration of metal ions (g mL^{-1}) in the leach liquor; V_c is the volume of the leach liquor (mL); M represents the weight (g) of dried nickeliferous laterite ore added in the reactor; and W_X is the mass percentage (wt%) of each metal in the nickeliferous laterite ores.

The leaching efficiency η_3 of each metal using limonite laterite ore atmospheric acid leaching liquors as lixiviant during the ferric chloride solution leaching process was calculated according to eqn (2).

$$\eta_3 = \frac{C_{1x} V_1 - C_{2X} V_2}{M' W_X} \times 100\% \quad (2)$$

where C_{1X} and C_{2X} represent the concentration of each metal ions (g mL^{-1}) in the leach liquor and lixiviant, respectively; V_1 and V_2 are the volumes (mL) of the leach liquor and lixiviant; M' represents the weight (g) of dried nickeliferous laterite ore added in the reactor; and W_X is the mass percentage (wt%) of each metal in the dried nickeliferous laterite ore.

The overall metal recovery for Ni, Co, Mn, and Mg and the overall leaching efficiency for iron were calculated according to eqn (3).

$$\eta_4 = \frac{C_{1X} V_1}{M_L W_{LX} + M' W_X} \times 100\% \quad (3)$$

where C_{1X} represents the concentration of metal ions (g mL^{-1}) in the leach liquor; V_1 is the volume (mL) of leach liquors; M_L and W_{LX} represent the weight (g) of dried limonite laterite ore used in atmospheric acid leaching process and the mass percentage of each metal (wt%), respectively; M' and W_X represent the weight (g) of dried nickeliferous laterite ores used in the ferric chloride solution leaching process and the mass percentage (wt%) of each metal, respectively.

3. Results and discussion

3.1 Elemental analysis and characterization of raw laterite ore

The chemical components of limonite and saprolite laterite ore, determined by X-ray fluorescence, are listed in Table 1. The contents of Fe and Mg in limonite laterite ore are 54.00% and 1.90%, respectively, while those in saprolite laterite ore are 15.00% and 11.1%, respectively. The nickel contents in limonite

Table 1 Chemical components of laterite ore of saprolite and limonite type (wt%)

	Fe	Mg	Ni	Co	Mn	Si	Al	Cr
Limonite	54.00	1.90	1.61	0.11	1.20	1.90	2.75	1.27
Saprolite	15.00	11.10	1.43	0.08	0.27	18.40	1.43	0.70

and saprolite laterite ore are 1.61% and 1.43%, respectively, which are typical low-grade nickeliferous laterite ores.

3.2 Atmospheric acid leaching process for limonite laterite ore

It is important to study the metal leaching behavior during atmospheric acid leaching of limonite laterite ore for the efficient and highly selective extraction of Ni and Co from nickeliferous laterite ore.[24,25] In the leaching process, valuable metals other than Fe, such as Ni, Co, and Mn, should be completely leached from limonite laterite ore. In addition, when the obtained leach liquors are used as lixiviant for saprolite or limonite laterite ore, it is necessary to ensure that residual H^+ ions and those that can be generated from the hydrolysis of Fe^{3+} ions are sufficient to efficiently leach Ni, Co, and Mn. Therefore, the influence of leaching parameters, including leaching temperature and time, acid concentration, and solid–liquid ratio, on leaching efficiency for each metal and concentrations of H^+ ions and Fe^{3+} ions in the leach liquors, was studied in the atmospheric acid leaching step. The results are presented in Fig. 2 and listed in Table 2.

As shown in Fig. 2(a), all the metal leaching efficiencies increase greatly with the increase in leaching temperature from 30 °C to 100 °C, indicating that metal dissolution is an endothermic reaction and higher leaching temperature favors metal leaching.[26] Taking into account the boiling point of hydrochloric acid solution, controllability of leaching temperature, and economy of practical operations, a leaching temperature of 100 °C was found to enable complete leaching of valuable metals from limonite laterite ore. This temperature was used in subsequent experiments to enhance the metal leaching efficiency while retaining sustainability and cost-effectiveness in practical applications. To determine the time required for efficient leaching of valuable metals from limonite laterite ore, a series of experiments were conducted; Fig. 2(b) shows the trend of metal leaching efficiency with the leaching time. In the initial 20 min, all the metals dissolved rapidly, and approximately 85.0% nickel, 80.0% cobalt, and 90.0% iron were leached. In the subsequent 40 minutes, all the metals dissolved slowly as the dissolution reactions approached equilibrium. To completely leach valuable metals, the leaching time was set at 60 min.

Furthermore, acid concentration and solid–liquid ratio play key roles in determining the metal leaching efficiency and the concentrations of Fe^{3+} and residual H^+ in the leach liquors.[27] Given that the hydrolysis of Fe^{3+} can produce H^+, this,

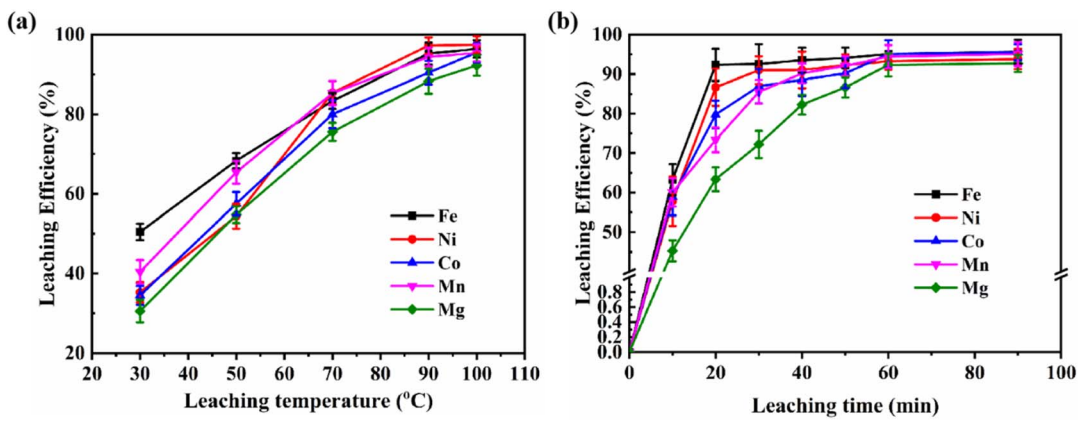

Fig. 2 Influence of leaching temperature (a) and time (b) on metal leaching efficiency from limonite laterite ore. Other leaching conditions: (a) acid concentration of 6 mol L^{-1}, solid to liquid ratio of 4 : 1 g mL^{-1} and leaching time of 120 min and (b) acid concentration of 6 mol L^{-1}, solid to liquid ratio of 4 : 1 g mL^{-1} and leaching temperature of 100 °C.

Table 2 Effects of acid concentration and solid–liquid ratio on metal leaching efficiency from limonite ore, and concentration of residual H^+ and Fe^{3+} in the leach liquors

		I	II	III	IV	V
Leaching conditions	Acid concentration (mol L^{-1})	3	4	4.8	6	8
	Solid to liquid ratio (g mL^{-1})	1 : 8	1 : 6	1 : 5	1 : 4	1 : 3
	Leaching temperature (°C)	100	100	100	100	100
	Leaching time (min)	60	60	60	60	60
Leaching efficiency (%)	Ni	97.3	97.2	97.5	97.0	97.0
	Co	95.3	95.2	95.3	95.2	95.0
	Mn	97.7	97.5	97.3	97.0	97.2
	Mg	90.3	92.5	93.6	94.8	95.6
	Fe	97.5	96.5	95.6	95.0	94.5
Concentration	Residual H^+ ions (mol L^{-1})	0.51	0.65	0.78	0.86	1.02
	Fe^{3+} ions (g L^{-1})	62.0	80.2	94.3	120.7	157.0

combined with the residual H^+ in leach liquors, would greatly affect the leaching efficiency and selectivity of Ni and Co from saprolite or limonite laterite ores during the ferric chloride solution leaching process. To realize efficient and highly selective leaching towards Ni and Co from the two types of nickeliferous laterite ore, a series of leach liquors was prepared from limonite ore using acid concentrations varying from 3 to 8 mol L^{-1} with solid–liquid ratios in the range of 1 : 8 g mL^{-1} to 1 : 3 g mL^{-1}. Under the designed leaching conditions, the leaching efficiency and the concentration of residual H^+ and Fe^{3+} ions in the leach liquors were investigated, as listed in Table 2. The leaching efficiencies of Ni, Mn, Co, and Mg remained almost constant over the range of conditions used. For the leach liquors obtained at different leaching conditions, the final iron concentrations were 62.0, 80.2, 94.3, 120.7 and 157.0 g L^{-1} and the residual H^+ ion concentrations were 0.51, 0.65, 0.78, 0.86 and 1.02 mol L^{-1}. It is proposed that these leach liquors can be used as lixiviant for the selective leaching of Ni and Co from nickeliferous laterite ore.

3.3 Ferric chloride solution leaching process for saprolite laterite ore

During the ferric chloride solution leaching process, Fe^{3+} was hydrolyzed to generate additional H^+ ions,[28] enabling nickel and cobalt rather than iron to be leached. Generally, the equilibrium of the leaching system depends on the hydrolysis of Fe^{3+} and the dissolution of metal elements, especially iron, indicating that the concentration of Fe^{3+} is important for leaching valuable metals. Furthermore, it was reported in our previous work that the form of iron ions in the liquors is closely related to the temperature and pH of the system.[29] As a result, the effects of concentration of Fe^{3+} ions, leaching temperature, liquid–solid ratio and residual acid concentration on the leaching efficiency for each metal, and the precipitation efficiency of Fe^{3+} ions, were investigated; the results are summarized in Fig. 3.

With the increase of leaching temperature from 120 °C to 200 °C, the leaching efficiencies of Ni^{2+} and Co^{2+} increase from 38.5% to 90.5%, and from 43.2% to 91.4%, respectively, and the precipitation efficiency of Fe^{3+} ions also increased from 47.5% to 91.3%. Higher leaching temperatures favor the hydrolysis of Fe^{3+} ions and produce more H^+ ions, which can promote the dissolution of Ni and Co from nickeliferous laterite ore.[30] Notably, when the leaching temperature was controlled at 180 °C, the precipitation efficiency of Fe^{3+} ions could exceed 90.0%. However, further increasing the leaching temperature had little effect on the precipitation efficiency of Fe^{3+} ions. Considering the greater energy consumption at higher temperatures, a leaching temperature of 180 °C was chosen.

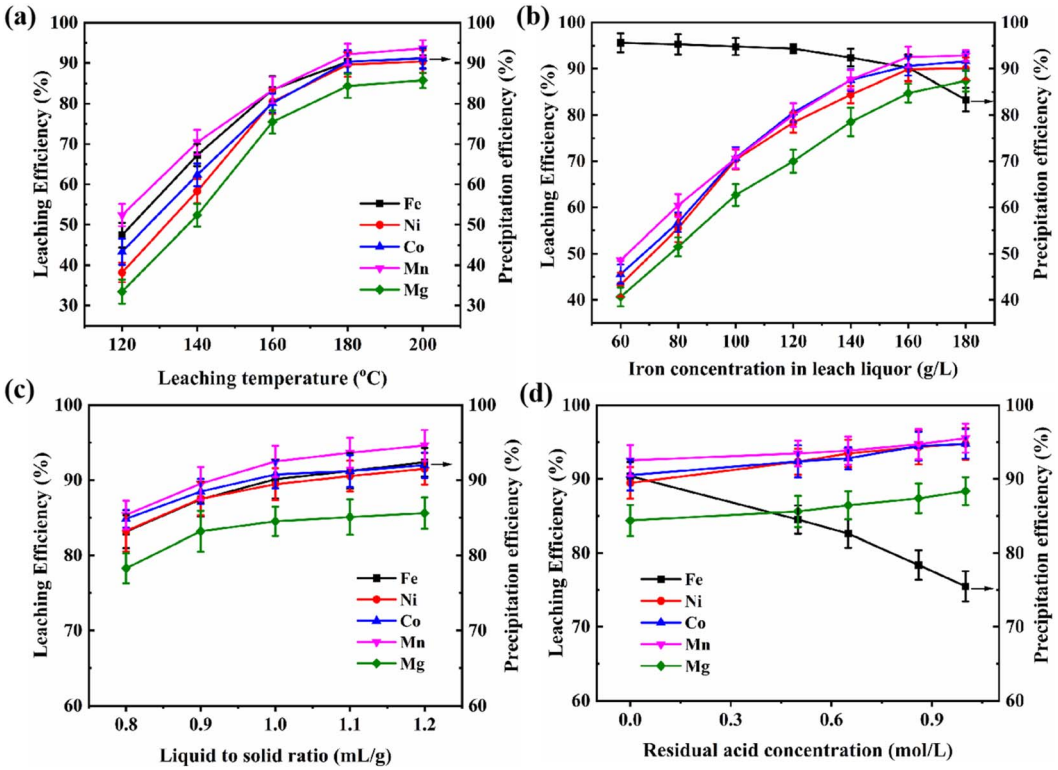

Fig. 3 Influence of leaching temperature (a) Fe ions concentration, (b) solid–liquid ratio (c) and acid concentration (d) on the leaching efficiency of valuable metals from saprolite laterite ore and precipitation efficiency of Fe^{3+}. Other leaching conditions: (a) iron concentration of 160 g L^{-1}, liquid to solid ratio of 1.0 mL g^{-1}, and leaching time of 180 min without residual acid; (b) leaching temperature of 180 °C, liquid to solid ratio of 1.0 mL g^{-1}, and leaching time of 180 min without residual acid; (c) leaching temperature of 180 °C, iron concentration of 160 g L^{-1}, and leaching time of 180 min without residual acid; and (d) leaching temperature of 180 °C, iron concentration of 160 g L^{-1}, liquid to solid ratio of 1.0 mL g^{-1}, and leaching time of 180 min.

The concentrations of Fe^{3+} ions in the liquors have a significant effect on the metal leaching efficiency and precipitation efficiency of Fe^{3+} ions, as shown in Fig. 3(b). Higher concentrations of Fe^{3+} ions can produce more H^+ ions due to the hydrolysis of Fe^{3+} ions, thereby improving the leaching efficiency of each metal besides iron. As the concentration of Fe^{3+} ions is increased from 60 to 180 g L^{-1}, the leaching efficiency for Ni^{2+} increases from 43.5% to 89.8%, and the leaching efficiency for Co^{2+} increases from 45.5% to 91.5%. However, the precipitation efficiency of Fe^{3+} ions decreases from 95.3% to 83.6%. To selectively leach Ni and Co, the optimized concentration of Fe^{3+} ions was controlled at 160 g L^{-1}.

To determine the influence of liquid–solid ratio on metal leaching efficiency and leaching selectivity towards Ni and Co over Fe, a series of leaching experiments with liquid–solid ratio varying from 0.8 to 1.2 mL g^{-1} were carried out under a leaching temperature of 180 °C and an Fe^{3+} concentration of 160 g L^{-1}. The results are shown in Fig. 3(c). Increasing the liquid–solid ratio, especially from 0.8 to 1.0 mL g^{-1}, can promote valuable dissolution of metals other than iron. Further increasing to 1.1 or higher had no significant influence on the leaching efficiency of valuable metals. As a result, the liquid–solid ratio was controlled at 1.0 mL g^{-1}.

As proposed initially, the atmospheric acid leaching liquors of limonite laterite ore are used as lixiviant for nickeliferous laterite ore during the ferric chloride solution leaching process. Notably, unreacted acid also exists in the leach liquors. Hence, it is necessary to investigate the effect of the concentration of residual acid on the metal leaching efficiency and nickel leaching selectivity; the results are shown in Fig. 3(d). Similar to the effect of Fe^{3+} ions, with increasing concentration of acid from 0 to 1.0 mol L^{-1}, the Ni^{2+} leaching efficiency increases slightly from 89.5% to 94.8% while the precipitation efficiency of Fe^{3+} ions decreases from 90.2% to 75.2%. For efficient and selective leaching of Ni and Co over Fe, the acid concentration in the liquors should therefore be maintained at less than 0.65 mol L^{-1}.

Based on the above experiments, the leaching efficiencies of Ni^{2+}, Mn^{2+}, Co^{2+}, and Mg^{2+} were 89.5%, 92.5%, 90.8% and 84.5%, respectively, while the precipitation efficiency of Fe^{3+} was 90.2% under the optimized leaching conditions ($T = 180$ °C, $CFe^{3+} = 160$ g L^{-1}, L/S = 1.0 mL g^{-1} and $CH^+ < 0.65$ mol L^{-1}). As shown in Fig. 3(b) and (d), the concentration of Fe^{3+} has a significant influence on the leaching efficiency of Ni^{2+} and Co^{2+}, and has a relatively small influence on the precipitation efficiency of Fe^{3+}, while the acid concentration has the opposite effects. To obtain high leaching efficiency and relatively high selectivity, leach liquor No. V (see Table 2) was chosen as the ferric chloride-rich solution for the leaching of saprolite laterite ore. The leaching results under different conditions are summarized in Table 3. With the leaching temperature increasing from 160 °C to 200 °C, the leaching efficiency for Ni^{2+} and Co^{2+} increases from about 90.0% to 94.0% while the precipitation efficiency of Fe^{3+} increases from 60.5% to 82.3%, implying that it is feasible to leach Ni and Co over Fe efficiently and selectively from nickeliferous laterite ore with limonite and saprolite types using a combined atmospheric acid leaching-ferric chloride solution leaching process.

3.4 Ferric chloride solution leaching process for limonite laterite ore

As shown in Table 1, there are significant differences in the chemical compositions between limonite and saprolite laterite ores; especially regarding the contents of iron and magnesium. As a result, the effects of leaching parameters, including leaching temperature, concentration of Fe^{3+} ions, liquid to solid ratio, and acid concentration, on leaching efficiency and selectivity towards Ni and Co over Fe from limonite laterite ore during the ferric chloride solution leaching process were also studied. The results are summarized in Fig. 4.

As shown in Fig. 4, the changes in the leaching efficiency and selectivity towards Ni and Co with the leaching parameters for limonite laterite ore show similar trends to those for saprolite laterite ore. However, the magnesium content in limonite laterite ore is much less than that in saprolite laterite ore, leading to an increase in the required concentration of Fe^{3+} ions in the lixiviant. The optimum leaching conditions for limonite laterite ore were determined to be a leaching temperature of 180 °C, liquid–solid ratio of 1.0 mL g^{-1}, Fe^{3+} concentration of 100 g $L^{-1}$and acid concentration of 0.5 mol L^{-1}. Under these leaching conditions, the leaching efficiencies of Ni^{2+}, Mn^{2+}, Co^{2+}, and Mg^{2+} were 93.8%, 93.6%, 93.5% and 89.5%, respectively, and the precipitation efficiency of Fe^{3+} ions was 87.5%.

Table 3 Leaching of saprolite laterite ore using the atmospheric acid leaching liquor (No. V listed in Table 2) of limonite laterite ore at various leaching temperatures

		I	II	III
Leaching conditions	Iron concentration (g L^{-1})	157.0	157.0	157.0
	Residual acid concentration (mol L^{-1})	1.02	1.02	1.02
	Liquid to solid ratio (mL g^{-1})	1.0	1.0	1.0
	Leaching time (min)	180	180	180
	Leaching temperature (°C)	160	180	200
Leaching efficiency (%)	Ni	89.3	93.2	94.5
	Co	90.2	93.8	94.8
	Mn	91.2	95.6	96.2
	Mg	80.1	89.2	90.8
Precipitation efficiency (%)	Fe	60.5	74.6	82.3

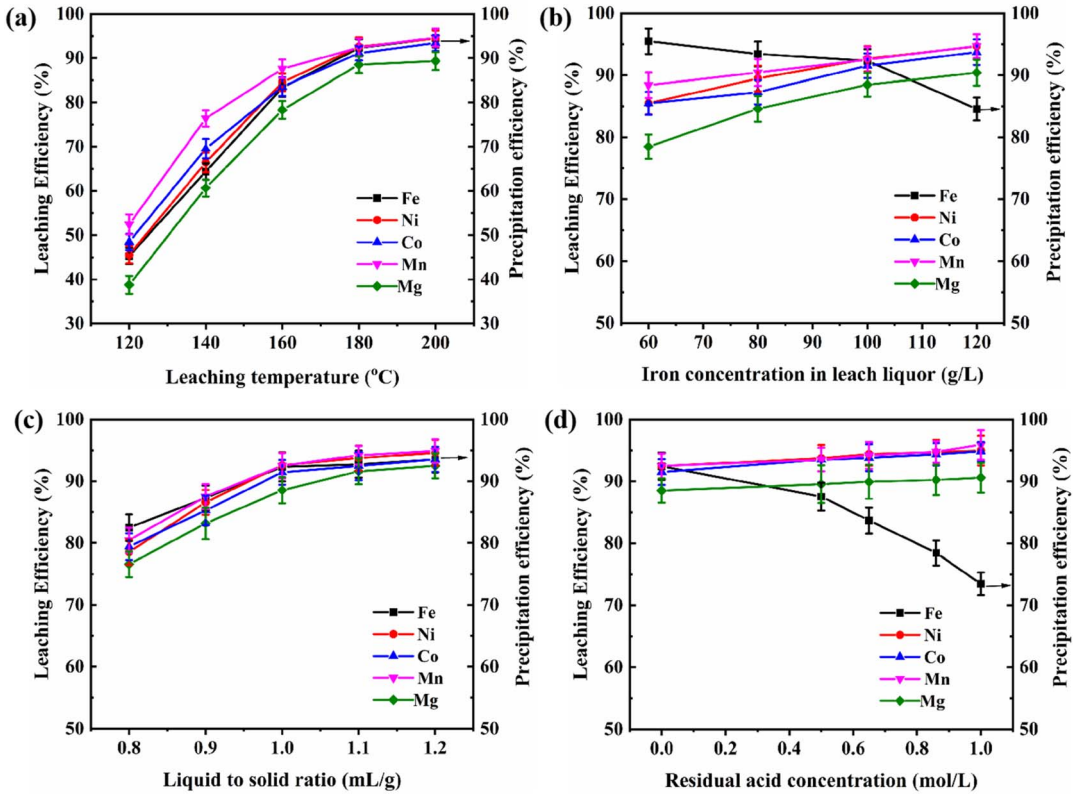

Fig. 4 Influence of leaching temperature (a), iron ion concentration (b), liquid to solid ratio (c) and acid concentration (d) on leaching efficiency of valuable metals from limonite laterite ore and the precipitation efficiency of Fe^{3+}. Other leaching conditions: (a) iron concentration of 100 g L^{-1}, liquid to solid ratio of 1.0 mL g^{-1}, and leaching time of 180 min without residual acid; (b) leaching temperature of 180 °C, liquid to solid ratio of 1.0 mL g^{-1}, and leaching time of 180 min without residual acid; (c) leaching temperature of 180 °C, iron concentration of 100 g L^{-1}, and leaching time of 180 min without residual acid; and (d) leaching temperature of 180 °C, iron concentration of 100 g L^{-1}, liquid to solid ratio of 1.0 mL g^{-1}, and leaching time of 180 min.

Based on these results, leach liquors No. II and III (as listed in Table 2) were also chosen as the lixiviant for ferric chloride solution leaching from limonite laterite ore. The leaching efficiency of Ni, Mn, Co, and Mg, and the precipitation of Fe, are listed in Table 4. It was found that efficient and selective leaching of Ni and Co (about 90.0%) over Fe (precipitation efficiency of around 85.0%) from limonite laterite ore could be achieved.

3.5 Leaching kinetics

Understanding leaching kinetics is essential for controlling the $FeCl_3$ leaching of laterite ore, which follows a fluid–solid reaction mechanism. The shrinking-core model, one of the most common frameworks for describing the fluid–solid reaction kinetics of dense (*i.e.*, non-porous) particles, posits that the overall reaction rate is governed by one of three steps: diffusion through the fluid boundary layer, diffusion through the solid-

Table 4 Leaching results of limonite laterite ore using atmospheric acid leaching liquors (No. II and III listed in Table 2) of limonite laterite ore under various leaching conditions

		I	II	III
Leaching conditions	Iron concentration (g L^{-1})	80.2	94.3	94.3
	Residual acid concentration (mol L^{-1})	0.65	0.78	0.78
	Leaching temperature (°C)	180	180	200
	Liquid to solid ratio (mL g^{-1})	1.0	1.0	1.0
	Leaching time (min)	180	180	180
Leaching efficiency (%)	Ni	89.8	93.2	94.8
	Co	90.3	93.6	95.2
	Mn	91.5	95.4	96.6
	Mg	86.5	90.3	92.3
Precipitation efficiency (%)	Fe	85.4	82.3	88.9

product (or unreacted-core) layer on the particle surface, or the chemical reaction at the interface of the unreacted core. Identifying which step controls the rate allows the operating conditions to be optimized and significantly improves process efficiency.

For the kinetics of metal dissolution, two previously established shrinking-core models, namely the reaction-controlled model and the Ginstling-Brounstein model,[31] were used; these models can be expressed as eqn (4) and (5), respectively:

$$1-(1-x)^{\frac{1}{3}}=kt \tag{4}$$

$$1-\frac{2}{3}x-(1-x)^{\frac{2}{3}}=kt \tag{5}$$

where x is the fractional leaching of Ni at time t, and k is the overall rate constant. Note that eqn (4) assumes that the rate-controlling step is the chemical reaction that occurs at the unreacted core, whereas eqn (5) assumes that it is diffusion through the product layer.

Fig. 5(a) and (d) illustrate the ferric chloride leaching experiments conducted at a liquid-to-solid ratio of 1.0 and initial Fe^{3+} concentrations of 157 g L^{-1} (for saprolite laterite ore) and 94.3 g L^{-1} (for limonitic laterite ore), across various temperatures and leaching times. Kinetic analysis based on the experimental data for Ni leaching from the laterite ore revealed that the Ni leaching rate increases significantly with elevated temperature and extended leaching time. The experimental data were fitted to eqn (4) and (5), and the rate constants (k) at different temperatures were calculated using the slopes of the straight lines passing through the origin, with the correlation coefficients detailed in Table 5. Comparative analysis of the fitting results for different control models indicates that the diffusion control model through the product layer yields the highest correlation coefficient between the fitted values and the experimental values. This suggests that the rate of the leaching reaction is primarily controlled by the diffusion process through the product layer.

The apparent rate constants can be utilized to determine the activation energy, E, in accordance with Arrhenius' Law, as described by eqn (6):

$$k=k_0e^{-\frac{E}{RT}} \tag{6}$$

Arrhenius analysis yields apparent activation energies of 12.8 kJ mol^{-1} for Ni leaching from saprolite laterite and 12.6 kJ mol^{-1} for limonite laterite under $FeCl_3$ treatment. Because mixed-control processes typically exhibit activation energies of 12–20 kJ mol^{-1}, these values indicate that Ni leaching is governed by both the surface chemical reaction and diffusion through the product layer.[32]

3.6 Mechanisms for efficient and selective leaching of Ni and Co

According to the above experimental results, it was found that efficient and selective leaching of Ni and Co (above 90%) over Fe (about 80.0% precipitation efficiency) from limonite and saprolite laterite ores could be realized using a combined atmospheric acid leaching-ferric chloride solution leaching process. To reveal the mechanisms for efficient and selective

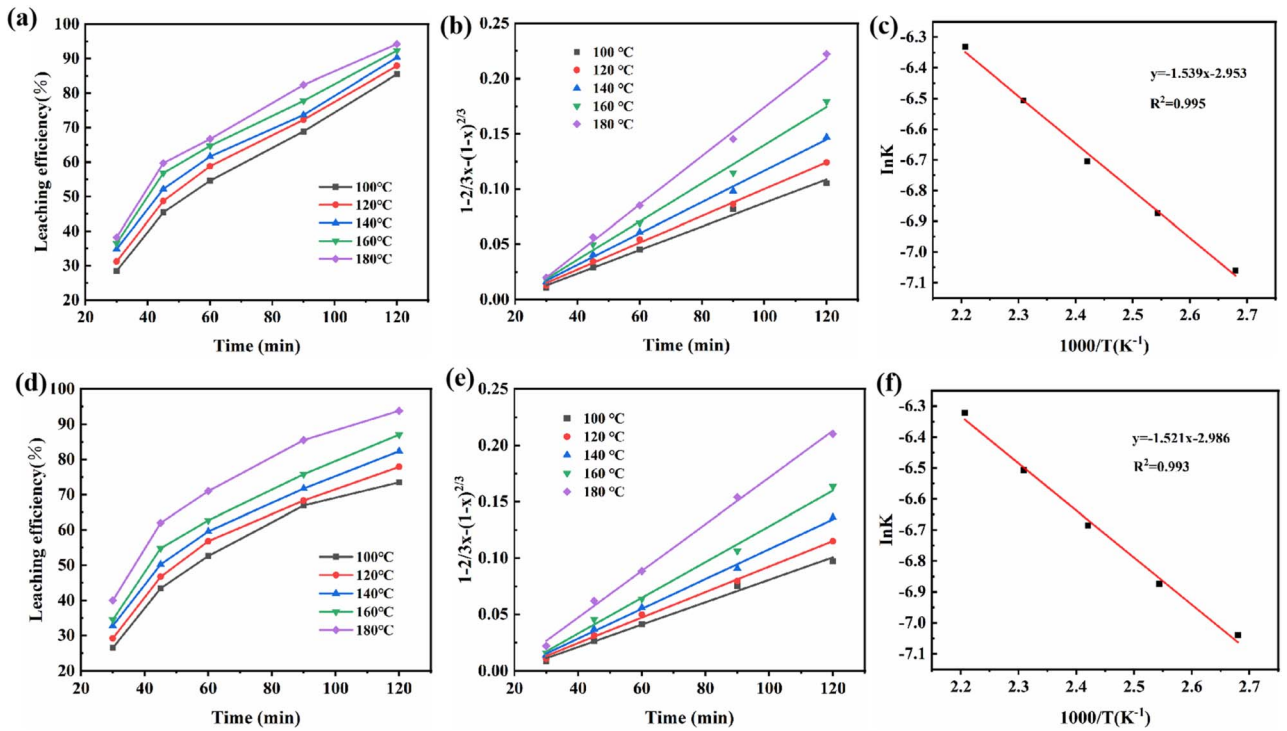

Fig. 5 Kinetic analysis of Ni leaching: (a–c) saprolite laterite and (d–f) limonite laterite nickel ore.

Table 5 Rate constants k and correlation coefficients R^2 for the leaching of Ni at different temperatures for the chemical reaction controlled model and the diffusion through the product layer model

	Saprolite laterite				Limonite laterite			
	Diffusion through the product layer		Chemical reaction		Diffusion through the product layer		Chemical reaction	
	$1 - 2/3x - (1-x)^{2/3}$		$1-(1-x)^{1/3}$		$1 - 2/3x - (1-x)^{2/3}$		$1-(1-x)^{1/3}$	
	k	R^2	k	R^2	k	R^2	k	R^2
100	0.000876	0.99036	0.003119	0.95677	0.000812	0.99038	0.097538	0.95461
120	0.001035	0.99684	0.003451	0.96923	0.000959	0.99694	0.006491	0.96684
140	0.001225	0.99632	0.003838	0.98212	0.001134	0.99661	0.006858	0.98007
160	0.001494	0.9903	0.004378	0.98267	0.001361	0.9926	0.00725	0.98002
180	0.001851	0.99607	0.005108	0.98953	0.001751	0.99652	0.00775	0.97907

leaching of Ni and Co, the XRD patterns of the leach residues of saprolite and limonite laterite ore after the ferric chloride solution leaching process were recorded, as shown in Fig. 6. It was found that hematite (Fe_2O_3) is the main mineral phase in the leach residues after the ferric chloride solution leaching process for both saprolite and limonite laterite ore. Goethite (FeOOH) in the leach residue of limonite laterite ore is likely the unreacted part of raw ore, which can be proved by the incomplete leaching of iron during the acid leaching process. In addition, hematite is easier to form than goethite at temperatures of 180–200 °C, further confirming the above conclusion regarding the source of the goethite (FeOOH) in the leach residue.

Fig. 7 displays the FTIR spectra of the leaching residues from saprolite (a) and limonite laterite ore (b). A characteristic band corresponding to the stretching vibration of –OH groups is observed at approximately 3161 cm^{-1} and 3425 cm^{-1}, whereas the band at 1630 cm^{-1} is attributed to the bending vibration of water molecules δ(H–O–H).[33] The sharp band observed within the range of 1031–1038 cm^{-1} is attributed to the asymmetric stretching vibrations of O–Si–O bonds. Additionally, the distinct bending vibrations of the O–Si–O groups are evident at 471–485 cm^{-1} and 905 cm^{-1}.[34] The bands at 800 cm^{-1} and 805 cm^{-1} are due to the bonds between H and O.[35] The peaks observed around 563 cm^{-1} are attributed to the bending vibrations of Fe–O bonds, thus indicating the presence of Fe_2O_3.[36] It was observed that the absorption peak corresponding to the bending mode of HO–Mg, appears around 620 cm^{-1} in the spectra of the ore. This peak shifts to 560 cm^{-1} in the leach residue. Additionally, the peaks gradually intensify after leaching, suggesting that the binding state of the OH group within the serpentine structure is altered due to the disordering of the local structure around metal ions.[37] From the SEM images (Fig. 8), it is observed that the leach residues contained spherical and lamellar structures, which are likely to be $FeCl_4^-$ complexes or aggregates of other metal compounds. Additionally, the FTIR spectra showed a broad absorption peak at 3425 cm^{-1} in the leach residues, which is characteristic of O–H stretching vibrations, indicating the presence of hydroxyl functional groups. The presence of these hydroxyl groups supports the theoretical reaction pathways for $FeCl_4^-$ hydrolysis and nickel mineral dissolution. As reported previously,[38,39] Fe^{3+} exists in the form of $FeCl_4^-$ in hydrochloric acid solution systems. The reaction mechanisms can be described by eqn (7)–(9). During the atmospheric acid leaching process, goethite (FeOOH) reacts with H^+ to generate Fe^{3+} ions in the leach

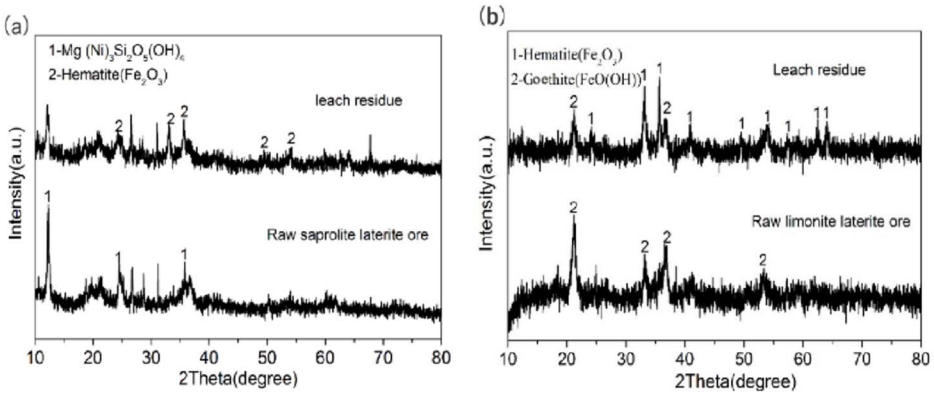

Fig. 6 XRD patterns of nickeliferous laterite ore with saprolite (a) and limonite types (b) and leach residues of saprolite (a) and limonite laterite ore (b) after the ferric chloride solution leaching process under the leaching conditions II as listed in Tables 3 and 4, respectively.

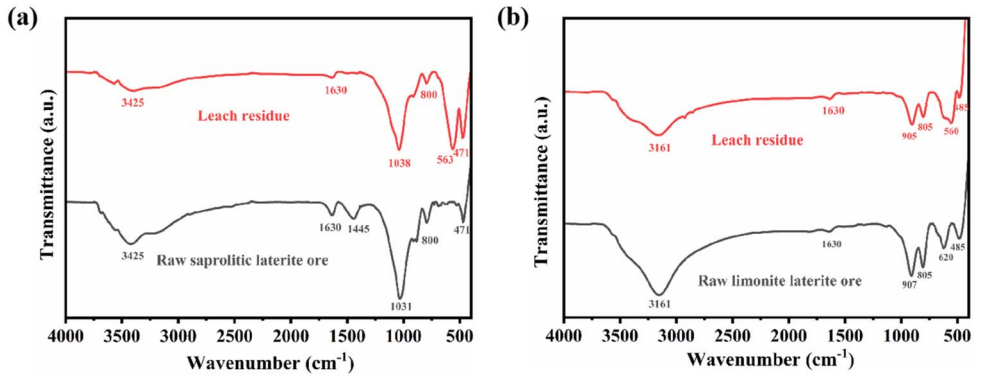

Fig. 7 FTIR spectra of nickeliferous laterite ore with saprolite (a) and limonite types (b), and leach residues of saprolite (a) and limonite laterite ore (b) after the ferric chloride solution leaching process under the leaching conditions II as listed in Tables 3 and 4, respectively.

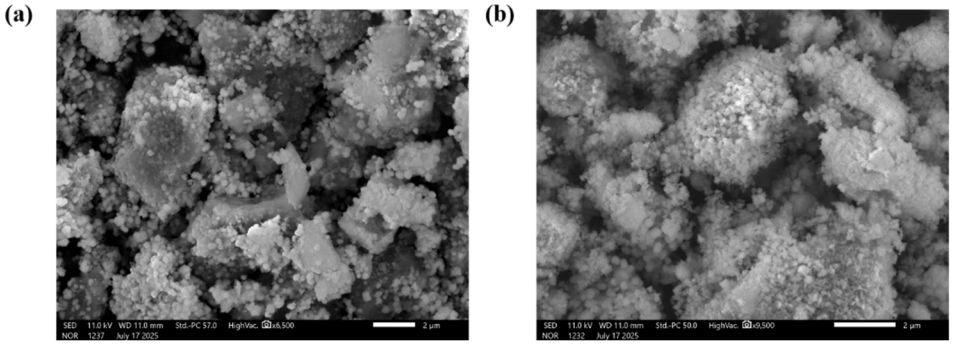

Fig. 8 SEM images of nickeliferous laterite ore with saprolite (a) and limonite types (b), and leach residues of saprolite (a) and limonite laterite ore (b) after the ferric chloride solution leaching process under the leaching conditions II as listed in Tables 3 and 4, respectively.

liquors, as given by eqn (7), resulting in simultaneous leaching of nickel and cobalt. During the ferric chloride leaching process, $FeCl_4^-$ in the lixiviant is hydrolyzed to transform into hematite and simultaneously generate H^+ ions, according to eqn (8). When sufficient H^+ ions are generated in the lixiviant, serpentine ($Mg_3Si_2O_5(OH)_4$) in saprolite laterite ore or goethite in limonite laterite ore react with the H^+ ions to leach nickel and cobalt, as shown in eqn (7) and (9). In fact, the hydrolysis reaction for Fe^{3+} takes place when residual H^+ is consumed up to a certain amount in the atmospheric acid leaching liquor, leading to efficient and selective leaching of Ni and Co from limonite and saprolite laterite ore.

$$FeOOH + 3H^+ \rightarrow Fe^{3+} + 2H_2O \quad (7)$$

$$2FeCl_4^- + 3H_2O \rightarrow Fe_2O_3 + 6H^+ + 8Cl \quad (8)$$

$$Mg_3Si_2O_5(OH)_4 + 6H^+ \rightarrow 3Mg^{3+} + 2SiO_2 + 5H_2O \quad (9)$$

3.7 Metal recovery and process evaluation

To determine the leaching selectivity, the leaching ratios of Ni/Fe and Co/Fe were calculated; the results are shown in Fig. S1. As the temperature increases, the dissolution efficiencies of Ni and Co accelerate significantly, while Fe is more prone to hydrolyze and precipitate, leading to an increase in the leaching ratios of Ni/Fe and Co/Fe. When the Fe^{3+} concentration is low to moderate, an appropriate amount of Fe^{3+} aids in the complexation and dissolution of Ni and Co, but excessive concentration leads to inhibition due to Fe competition with the valuable metals. A larger liquid-to-solid ratio not only improves the contact efficiency between H^+/Fe^{3+} and the ore, but also promotes the relative enrichment of Ni and Co by diluting the Fe concentration. The residual acid concentration exhibits a "promoting-inhibiting" trend, with the optimal acidity range being 0.3–0.6 mol L^{-1}. Under the optimal conditions, the Ni/Fe and Co/Fe ratios for saprolite-type laterite ore reached 13.8 and 14.2, respectively, while for limonite-type laterite ore, the ratios were further increased to 18.2 and 18.1, respectively, demonstrating that the process exhibits better leaching selectivity for limonite-type laterite nickel ore.

To ensure the efficacy of Ni and Co recovery, we further examined the potential interference from Al and Cr leaching. The concentrations and leaching rates of Al and Cr in the ferric chloride leachate were measured, as shown in Fig. 9. Under the current conditions, saprolite laterite yielded leaching rates of

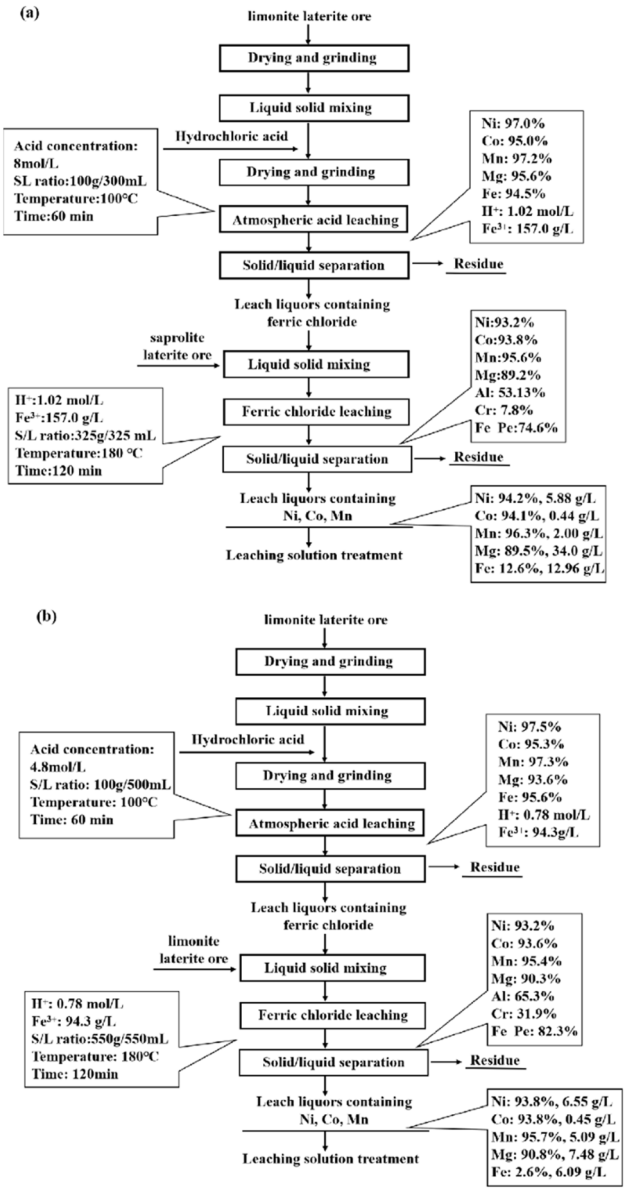

Fig. 9 Summary of the leaching efficiency, migration and transformation behaviors of each metal for the combined leaching process of limonite–saprolite (a) and limonite–limonite (b) under the optimum conditions.

53.13% for Al Cr and 7.8% for Cr, while those of limonitic laterite reached 65.3% and 31.9%, respectively. Chromite (partially replaced by Al, Fe, and Al/Si) is partially dissolved by HCl,[33] which liberates Al and Cr ions that then compete with nickel and cobalt for complexation or co-precipitation during downstream separation—crowding out extractant or adsorbent sites and impairing both recovery efficiency and product purity. To address this, we optimized key leaching parameters (acid concentration, ferric ion dosage, liquid-to-solid ratio, temperature, and time) to suppress Al and Cr dissolution while maintaining high nickel and cobalt recoveries. In future work, the pH value of leachate will be adjusted to 4.5–5.0 to precipitate Al and Cr hydroxides by sedimentation, and the use of amino- or carboxyl-functionalized adsorption resins and weakly acidic ion-exchange resins to selectively remove residual Al and Cr will be evaluated, targeting less than 1% remaining and ensuring high-purity nickel and cobalt separation.

Under the combined optimum leaching conditions for limonite–saprolite laterite ore and limonite–limonite laterite ore, the leaching efficiency, migration, and transformation behavior for each metal are summarized in Fig. 9. The metal recoveries of Ni^{2+} and Co^{2+} from limonite–saprolite laterite ore were calculated as 94.2% and 94.1%, respectively, while those from limonite–limonite laterite ore were 93.8% and 93.8%, respectively. At the same time, the metal recovery for manganese was higher than 90.0%. Furthermore, the concentrations of Fe^{3+} in the leach liquors obtained from sequential limonite–saprolite laterite ore and limonite–limonite laterite ore were 12.96 g L^{-1} and 6.09 g L^{-1}, respectively, and the corresponding leaching efficiencies of iron were 12.6% and 2.6%, respectively, which are similar to the outcomes of leaching by the pressure acid leaching process (250–270 °C and 4–5 MPa).[40] However, the leaching temperature and leaching pressure for the ferric chloride leaching are 180 °C and 0.9 MPa, which are much lower than the leaching conditions of the pressure acid leaching process. Furthermore, the HCl acid consumptions for limonite–saprolite laterite ore and limonite–limonite laterite ore are 420 and 300 kg t^{-1}, respectively, which are much lower than that for the pressure acid leaching process (600–900 kg t^{-1}). In short, efficient and selective leaching of Ni and Co from nickeliferous laterite ore was realized by the proposed combined atmospheric acid leaching-ferric chloride solution leaching process.

The proposed process significantly outperforms high-pressure acid leaching and pyrometallurgical processes in terms of energy consumption,[41] material consumption, and environmental friendliness, particularly for high-iron and low-magnesium laterite nickel ore; a detailed comparison is shown in Table 6. This process achieves waste minimization through mild reaction conditions, acid regeneration closed-loop circulation, and iron slag resource utilization. The iron slag precipitates in the form of Fe_2O_3, which can be directly used as a raw material for iron smelting, and the amount of slag per ton of nickel is reduced to 0.5–1 ton. At the same time, the closed-loop circulation of hydrochloric acid avoids waste acid discharge, reduces the risk of heavy metal wastewater, and significantly reduces carbon emissions to about 13.7 tons CO_2 per ton of nickel. However, the limitation of this process lies in equipment corrosion, which requires the use of corrosion-resistant materials such as Hastelloy, increasing the initial investment. In addition, the adaptability to high-magnesium laterite ore is poor, and the acid consumption increases significantly when the magnesium content is high, requiring pre-treatment to remove magnesium. In the future, the economic core of the process will depend on the improvement of hydrochloric acid regeneration efficiency, while also needing to overcome the bottleneck of high-magnesium ore pre-treatment and corrosion-resistant material costs.

Table 6 Energy consumption, material consumption, and environmental benefits comparison of the combined atmospheric acid leaching-chloride iron extraction and high-pressure acid leaching in laterite nickel ore processing

	Energy consumption characteristics		Material efficiency		Economic evaluation				Environmental benefits	
Experimental method	Reaction conditions	Comprehensive energy consumption	Acid consumption	Metal extraction features	Investment cost per ton of nickel	Acid consumption cost	Operating cost	Applicable ore types	Waste minimization	Pollution control
Atmospheric acid leaching – chloride iron extraction	80–150 °C (Normal pressure)	Low, no high-pressure equipment required, and equipment operation energy consumption is low	300–450 kg t^{-1} of ore	Cl^- enhances nickel dissolution, reduces impurity co-dissolution	Approximately 1.5 times the cost of electric furnace process	Low (acid recycling possible)	Low due to minimal neutralization and iron removal requirements	Limonite-type (high iron, low magnesium)	Slag utilization rate >90%, nickel slag 0.5–1 ton	A closed-loop hydrochloric acid cycle avoids waste acid discharge; carbon emissions are 13.7 tons CO_2 per ton of nickel, which is 70% lower than the blast furnace process
High-pressure acid leaching (HPAL)	245–260 °C; 4–5 MPa	High, requires high-pressure equipment and has high energy consumption for equipment operation and heating	600–900 kg t^{-1} of ore	Requires handling of large amounts of iron impurities, significant co-dissolution of impurities	More than three times the cost of electric furnace process	High (sulfuric acid cannot be recycled)	High due to the need for neutralization and iron removal	High-grade ore	Slag utilization rate <100%, nickel slag 120 tons	Potential heavy metal wastewater risk, high carbon footprint

4. Conclusions

Efficient and selective leaching of Ni and Co from limonite–saprolite and limonite–limonite laterite ore could be realized through the developed combined atmospheric acid leaching-ferric chloride solution leaching process. During the atmospheric acid leaching process, approximately 95.0% of valuable metals other than iron can be leached into the leach liquors under the optimum leaching conditions, and leach liquors with iron concentrations varying from 60 to 157 g L^{-1} can be used as lixiviant for limonite or saprolite laterite ore during the ferric chloride solution leaching process. The leaching temperature and the concentrations of Fe^{3+} and H^{+} have significant effects on the leaching selectivity towards Ni and Co over Fe during the ferric chloride solution leaching process. When the leaching conditions were controlled at 180 °C for 120 min with iron concentrations of 160 and 100 g L^{-1} in the initial liquors for saprolite and limonite laterite ore, respectively, the leaching efficiency of Ni and Co from nickeliferous laterite ore exceeded 90.0% and the precipitation efficiency of Fe^{3+} was approximately 90.0%. For the overall leaching process, the leaching efficiencies of Ni and Co were above 90.0% while the leaching efficiency of Fe from limonite–saprolite laterite ore and limonite–limonite laterite ore were 12.6% and 2.6%, respectively. This study provides technical and theoretical support for the selective leaching of valuable metals over iron from polymetallic resources.

Author contributions

J. L. designed and performed the experiments, collected data, and drafted the initial manuscript. T. Y. conducted material characterization and leach residue analysis. C. L. performed mechanistic calculations and model construction. X. H. handled data analysis, statistical validation, and figure preparation. J. G. supervised the project, acquired resources, revised the manuscript, and managed submission.

Conflicts of interest

The authors declare no conflicts of interest.

Data availability

The authors confirm that the data supporting the findings of this study are available within the article and/or its SI. See DOI: https://doi.org/10.1039/d5ra04469c.

Acknowledgements

The work was financially supported by the National Natural Science Foundation of China (No. 22378244 and 51804192), Shanxi Province Youth Top notch Talent Project, and Shanxi Province Central Government Guided Local Science and Technology Development Fund Project (No. YDZJSX2022A004).

References

1 J. Guo, X.-R. Chen, S.-W. Han, Y. Yan and H.-J. Guo, *Int. J. Miner. Metall. Mater.*, 2020, **27**, 328–339.
2 C. Tan and C. Chen, *Angew. Chem., Int. Ed.*, 2019, **58**, 7192–7200.
3 M. H. Abdi and N. B. Ibrahim, *Phys. B Condens. Matter*, 2020, **581**, 411758.
4 W.-M. Liu, M.-L. Qin, L. Xu, S. Yi, J.-Y. Deng and Z.-H. Huang, *Trans. Nonferrous Metals Soc. China*, 2018, **28**, 1626–1631.
5 S. A. Gleeson, C. R. M. Butt and M. Elias, *SEG Discovery*, 2003, **54**, 1–18.
6 K. Wang, J. Wan, Y. Xiang, J. Zhu, Q. Leng, M. Wang, L. Xu and Y. Yang, *J. Power Sources*, 2020, **460**, 228062.
7 X. X. Wang, V. Prabhakaran, Y. He, Y. Shao and G. Wu, *Adv. Mater.*, 2019, **31**, 1805126.
8 A. A. Ali, E. El Fadaly and I. S. Ahmed, *Dyes Pigm.*, 2018, **158**, 451–462.
9 J. Xu, C.-m. Cao, P. Gu and L.-m. Peng, *Trans. Nonferrous Metals Soc. China*, 2020, **30**, 746–755.
10 P. Zhang, Q. Guo, G. Wei, L. Meng, L. Han, J. Qu and T. Qi, *Hydrometallurgy*, 2015, **157**, 149–158.
11 Q. Guo, J. Qu, B. Han, P. Zhang, Y. Song and T. Qi, *Miner. Eng.*, 2015, **71**, 1–6.
12 K. Liu, Q. Chen, H. Hu, Z. Yin and B. Wu, *Hydrometallurgy*, 2010, **104**, 32–38.
13 R. G. McDonald and B. I. Whittington, *Hydrometallurgy*, 2008, **91**, 35–55.
14 R. G. McDonald and B. I. Whittington, *Hydrometallurgy*, 2008, **91**, 56–69.
15 K. Wang, J. Li, R. G. McDonald and R. E. Browner, *Hydrometallurgy*, 2011, **109**, 140–152.
16 K. Wang, J. Li, R. G. McDonald and R. E. Browner, *Miner. Eng.*, 2018, **116**, 35–45.
17 P. Zhang, Q. Guo, G. Wei, J. Qu and T. Qi, *Hydrometallurgy*, 2015, **153**, 21–29.
18 B. Ma, W. Yang, Y. Pei, C. Wang and B. Jin, *Hydrometallurgy*, 2017, **169**, 411–417.
19 S. Cetintas, U. Yildiz and D. Bingol, *J. Clean. Prod.*, 2018, **199**, 616–632.
20 X. Zhai, Y. Fu, X. Zhang, L. Ma and F. Xie, *Hydrometallurgy*, 2009, **99**, 189–193.
21 S. Y. Tshipeng, A. TshamalaKaniki and M.-B. Kime, *J. Sustain. Metall.*, 2017, **3**, 823–828.
22 P. Zhang, L. Sun, H. Wang, J. Cui and J. Hao, *J. Clean. Prod.*, 2019, **228**, 1–7.
23 J. Li, D. Li, Z. Xu, C. Liao, Y. Liu and B. Zhong, *J. Clean. Prod.*, 2018, **179**, 24–30.
24 J. MacCarthy, A. Nosrati, W. Skinner and J. Addai-Mensah, *Hydrometallurgy*, 2016, **160**, 26–37.
25 W. Astuti, T. Hirajima, K. Sasaki and N. Okibe, *Hydrometallurgy*, 2016, **161**, 138–151.
26 G. Li, Q. Zhou, Z. Zhu, J. Luo, M. Rao, Z. Peng and T. Jiang, *J. Clean. Prod.*, 2018, **189**, 620–626.
27 B. Wang, L. Mu, S. Guo and Y. Bi, *Hydrometallurgy*, 2019, **183**, 98–105.

28 P. Zhang, Q. Guo, G. Wei, L. Meng, L. Han, J. Qu and T. Qi, *J. Clean. Prod.*, 2016, **112**, 3531–3539.
29 J.-m. Gao, M. Zhang and M. Guo, *Hydrometallurgy*, 2015, **158**, 27–34.
30 Z. Yu, K. Xie, W. Ma, Y. Zhou, G. Xie and Y. Dai, *Rare Met.*, 2011, **30**, 688–694.
31 C. K. Thubakgale, R. K. K. Mbaya and K. Kabongo, *Miner. Eng.*, 2013, **54**, 79–81.
32 P. Zhang, Q. Guo, G. Wei, L. Meng, L. Han, J. Qu and T. Qi, *Hydrometallurgy*, 2015, **157**, 149–158.
33 B. Wang, Q. Guo, G. Wei, P. Zhang, J. Qu and T. Qi, *Hydrometallurgy*, 2012, **129–130**, 7–13.
34 A. Hahn, H. Vogel, S. Andó, E. Garzanti, G. Kuhn, H. Lantzsch, J. Schüürman, C. Vogt and M. Zabel, *Sediment. Geol.*, 2018, **375**, 27–35.
35 N. Perrier, R. J. Gilkes and F. Colin, *Clays Clay Miner.*, 2006, **54**, 165–175.
36 J. Kugbe, N. Matsue and T. Henmi, *J. Hazard. Mater.*, 2008, **164**, 925–935.
37 Q. Zhang, K. Sugiyama and F. Saito, *Hydrometallurgy*, 1997, **45**, 323–331.
38 Z. Zhou, W. Qin, Y. Chu and W. Fei, *Chem. Eng. Sci.*, 2013, **101**, 577–585.
39 M. S. Sitze, E. R. Schreiter, E. V. Patterson and R. G. Freeman, *Inorg. Chem.*, 2001, **40**, 2298–2304.
40 D. H. Rubisov and V. G. Papangelakis, *Hydrometallurgy*, 2000, **58**, 89–101.
41 L. Shi, B. Ma, Z. Cao, J. Yu, F. He and C. Wang, *Miner. Eng.*, 2025, **227**, 109255.